Terrain Learning using Time Series of Ground Unit Traversal Cost

Miloš Prágr[0000−0002−8213−893X]* and Jan Faigl[0000−0002−6193−0792]

Faculty of Electrical Engineering, Czech Technical University in Prague,
Technicka 2, 166 27, Prague, Czech Republic
{pragrmi1,faiglj}@fel.cvut.cz
https://comrob.fel.cvut.cz

Abstract. In this paper, we concern learning of terrain types based on the traversal experience observed by a hexapod walking robot. The addressed problem is motivated by the navigation of unmanned ground vehicles in long-term autonomous missions in a priory unknown environments such as extraterrestrial exploration. In such deployments, the robotic vehicle needs to learn hard to traverse terrains to improve its autonomous performance and avoid possibly dangerous areas. We propose to utilized Growing Neural Gas for terrain learning to capture the robot experience with traversing the terrain and thus learn a classifier of individual terrain types. The classifier is learned using a real time-series dataset collected by a hexapod walking robot traversing various terrain types. The learned model can be utilized to predict the traversal cost of newly observed terrains to support decisions on where to navigate next.

1 Introduction

Traversal of different terrains is one of the main concerns for unmanned ground vehicles in long-term deployments such as data gathering, environment monitoring, search-and-rescue, or exploration missions. For example, the Mars rover Spirit got stuck in soft sand despite being navigated with human oversight [2]. Ground robot system deployments range from terrain classification approaches that use human terrain type labels [1,22] or distinguish non-traversable obstacles [13]; to self-supervised systems that autonomously learn terrain type classifiers [8]. Alternatively, the terrain traversability might be computed directly as a function of terrain appearance and geometry [24], measure robot performance [12], or evaluate the foothold configuration of a multi-legged robot [15].

Our particular research on terrain traversability is focused on deployments without a priory learning of the traversal costs, and we aim to support instant deployments of online learned models. In [20,21], we develop a robotic system that incrementally learns to predict power consumption-based traversal costs that are experienced by the robots over various traversed terrains. Besides, in [19], we deploy a robotic system that incorporates fully autonomous spatial exploration of the terrain with a simultaneous exploration of the underlying traversal

cost model of the traversed terrains, such that the learned cost model is instantaneously utilized in autonomous navigation to avoid costly terrains. Moreover, we investigate self-organizing neural network approaches in terrain classification and traversal cost prediction [5,4,18], namely variants of the Growing Neural Gas (GNG) [7], Self-Organizing Map (SOM) [11], and Improved Self-Organizing Incremental Neural Network (ISOINN) [23]. Although the previous results provide particular solutions experimentally verified in a series of deployments, they are limited to aggregated cost data that are driven by a spatial grid-based representation of the operational environment. However, the traversal cost is computed from a sequence of measurements. Therefore, the cost prediction can be based on direct employment of the input time series of the considered proprioceptive, but also exteroceptive measurements. Thus, in this paper, we report on our further research on terrain learning explicitly based on time series.

Time series data are already employed in many domains ranging from medicine [14,26] through handwriting [25] and gestures [17] to classification of physical activities [27]. Recently, machine learning approaches such as Support vector machines [9] and Deep convolutional neural networks [27] has been employed in time series classification. From the existing approaches, One-nearest-neighbor (1-NN) is a simple yet popular approach. When it is utilized with time-series data, the 1-NN can calculate the distance between time series measurements using the Dynamic Time Warping (DTW) [16], although the authors of [10] report in favor of the Euclidean distance. In [25], a semi-supervised 1-NN time series classifier is presented, and the authors of [26] demonstrate the speedup of 1-NN using numerous reduction. A combination of the k-NN with Growing Neural Gas (GNG) is presented in [17] to classify multi-channel time series.

In this paper, we report on the deployment of the GNG-based 1-NN terrain classifier that is learned using a time series dataset, and the proposed approach is compared to the baseline non-time series setup. Moreover, the learned classifier is employed in the prediction of the energy-based traversal cost. Finally, we investigate the representation of the robot proprioception as an aggregated cost computed over time series segments. In this case, the influence of the subsampling rates is investigated, and we report the computational efficiency of the proposed concise representation.

The paper is organized as follows. In Section 2, the utilized terrain traversal dataset is described in the context of the terrain classification and traversal cost prediction problems. The used GNG algorithm is described in Section 3, while Section 4 reports on the achieved results. The concluding remarks are in Section 5.

2 Time-Series Dataset and the Terrain Learning Problem

We address learning of terrain type classifiers using a dataset of terrain feature descriptors and multi-legged robot proprioceptive signals. The dataset is organized as time series sampled with 10 Hz. The time series is cut in 10 s long segments, where each segment represents a single locomotion gait cycle of the

robot. Hence, there are 101 data points in each segment. The segments are reported with 1 Hz to account for the different possible offsets with regards to the gait cycle. Furthermore, the baseline non-time series approach is represented as non-time series data points, where each non-time series data point corresponds to one time series segment.

Each data point (regardless of whether it is a part of the segment or a standalone, not time series point) comprises descriptors of the terrain shape and appearance coupled with the proprioceptive measurements of the robot power consumption. The terrain descriptors are based on the previous work [20], and each terrain descriptor characterizes the area of 0.2 m radius around the ground projection of the robot's body center of mass. The shape descriptors are determined from the eigenvalues of the covariance matrix of the surface points in the area as (f_5, f_6, f_7) presented in [13]. The appearance descriptors are the ab channel means of the Lab color space representation of the surface points in the area.

The instantaneous power consumption [12] signal is determined as

$$P_{in} = V \cdot I \quad [\mathrm{W}], \tag{1}$$

where V is the battery voltage and I is the instantaneous current measurement, which is sampled with 10 Hz. Besides the raw power consumption signal, the aggregated traversal cost c is determined as the total energy consumed over the given interval. The aggregated cost c over the interval between two consecutive power measurements is computed using the trapezoid integration rule

$$c(t_i, t_{i-1}) = (t_i - t_{i-1}) \frac{P_{in}(t_{i-1}) + P_{in}(t_i)}{2} \quad [\mathrm{J}], \tag{2}$$

where t_i and t_{i-1} are the corresponding sampling times, and $P_{in}(t_i)$ and $P_{in}(t_{i-1})$ are the respective power consumption measurements. Given the additive nature of the integration, it holds that

$$c(t_{i+1}, t_{i-1}) = c(t_{i+1}, t_i) + c(t_i, t_{i-1}) \quad [\mathrm{J}]. \tag{3}$$

Therefore, the traversal cost $c(T)$ over a segment T with 101 power measurements sampled with 10 Hz is defined as

$$c(T) = \sum_{i=1}^{100} c(t_{i+1}, t_i) | \{t_i\}_{i=1}^{101} \in T \quad [\mathrm{J}]. \tag{4}$$

In the considered dataset, we can distinguish two types of time series segments or non-time series points. The first type includes the time series segments T_{ts} with power measurements replaced by the aggregate traversal cost, which may be sampled at a lower frequency. Since each two subsampled points at t'_{j+1}, t'_j correspond to $k+1$ points $(t_i, ..., t_{i+k})$ in the raw 10 Hz time series, where $t'_{j+1} - t'_j = t_{i+k} - t_i$, the cost for the interval (t'_{j+1}, t'_j) between the points in T_{ts} is computed using (2) and (3) as

$$c(t'_{j+1}, t'_j) = \sum_{l=i}^{i+k-1} c(t_{l+1}, t_l) \quad [\mathrm{J}]. \tag{5}$$

(a) (b)

Fig. 1. (a) The utilized hexapod walking robot on the *cubes* terrain with *turf* terrain in the background; (b) and the overhead view of *cubes covered with black* terrain.

Therefore, the cost of the segment T_{ts} is the sum

$$c(T_{ts}) = \sum_{j=1}^{|T_{ts}|-1} c(t'_{j+1}, t'_j) | \{t_j\}_{j=1}^{|T_{ts}|} \in T_{ts} \quad [\mathrm{J}], \tag{6}$$

where $|T_{ts}|$ is the number of points in the subsampled time series. The second type is the non-time series data points, which represent the robot power consumption as the mean over the 10 s segment T_{point}

$$\hat{P}(T_{point}) = \frac{1}{101} \sum_{i=1}^{101} P_{in}(t_i) | \{t_i\}_{i=1}^{101} \in T_{point} \quad [\mathrm{W}], \tag{7}$$

and the aggregate cost over the 10 s long segment is thus approximated as

$$c(T_{point}) = 10\hat{P}(T_{point}) \quad [\mathrm{J}]. \tag{8}$$

The latter type has been utilized in our previous research reported in [4,20], and therefore, it is considered as the baseline approach.

The time-series dataset is collected by the small battery-powered hexapod walking robot shown in Fig. 1a that is controlled by adaptive locomotion control [3] capable of crawling rough terrains. The robot is guided over a set of human-labeled terrains that can be categorized as *flat* office ground, artificial *turf*-like carpet, *black* fabric, and wooden *cubes* of uneven height and slope. Two further terrain types are created as *cubes covered with turf* and *cubes covered with black* fabric, see Fig. 1b. Thus, each time series segment or its corresponding non-time series point T is accompanied by a human terrain label. The performance of the terrain classifier $\mathcal{C}$ can be determined as the number of correct classifications further denoted as correctness:

$$correctness(\mathcal{T}, \mathcal{C}) = \frac{1}{|\mathcal{T}|} \sum_{T \in \mathcal{T}} \begin{cases} 1 & \text{if} \quad \text{classify}(T, \mathcal{C}) = label(T) \\ 0 & \text{otherwise} \end{cases} 100\%, \tag{9}$$

where $\mathcal{T}$ is the test set of time series segments T with hidden labels $label(T)$. The traversal cost predictor $\mathcal{I}$ is evaluated with regards to the RMSE

$$RMSE(\mathcal{T}, \mathcal{I}) = \sqrt{\frac{\sum_{T_{terrain} \in \mathcal{T}} (predict(T_{terrain}, \mathcal{I}) - c(T))^2}{|\mathcal{T}|}}, \qquad (10)$$

where the terrain descriptor segment $T_{terrain}$ is the queried time series segment T stripped of the proprioceptive measurements; and $c(T)$ is its ground truth traversal cost computed computed over the testing data using (4).

The dataset is organized into six sequences called trails, where each trail corresponds to one terrain. The individual segments or non-time series points in each trail are ordered as the robot has experienced them. Therefore, the dataset mimics the order of data in incremental learning. The learning set is created as the first two-thirds of each trail, and the last third is reserved for testing with regards to (9) and (10).

3 Time Series Learning Growing Neural Gas

A Growing Neural Gas (GNG) scheme [7] is employed to learn a classifier of terrain traversal time series segments. The baseline non-time series classifiers are also learned using this scheme, i.e., they are considered to be time series with one point. For the sake of brevity, the herein presented description of the GNG is limited to the use of the GNG in the classification scheme, which is summarized in Alg. 1. We kindly refer the reader to [7] or [6] for a detailed description of the GNG algorithm.

The herein reported results are based on the Online Semi-Supervised Multi-Channel Growing Neural Gas (OSSMGNG) [17]. Similarly to the OSSMGNG, the proposed approach utilizes separate GNG structures learned for each of the particular classes. However, the dataset presented in Section 2 comprises time series segments with a fixed size, and there is no need to map unknown dimensions as in [17]. Thus, we employ the Euclidean $L2$-norm to compute the distance between the time series segments, because unlike the therein used DTW scheme, the Euclidean norm can be computed in $\mathcal{O}(d)$, where d is the data dimensionality. In the case when some of the dimensions of the segment are missing, i.e., during the inference, the distance is computed using only the known dimensions.

The GNG is updated in supervised way, i.e., the time series segment is accompanied by the terrain label, and the respective class network is updated with $\epsilon_{winner} = 0.1$, $\epsilon_{neighbor} = 0.01$, $\alpha_{split} = 0.5$, $\alpha_{error} = 0.99$, $a_{max} = 50$, and $\lambda = 30$, see **Supervised Update** procedure in Alg. 1. Unlabeled segments are classified by finding the class of its nearest neighbor among nodes from all the GNGs (**Classify** procedure in Alg. 1).

Finally, the learned classifier is used to infer missing dimensions of the segment $T_{terrain}$ using the 1-NN approach as follows. First, $T_{terrain}$ is classified; then, the nearest neuron within the respective GNG class is found, and the

Algorithm 1: Time series learning Growing neural gas

▶ **Supervised Update** $(T, label, \mathcal{G})$

Input: T – time series segment, $label$ – segment label, $\mathcal{G}$ - set of GNG models for the individual terrain classes

```
G ← 𝒢[label]                    // Select the respective GNG model for label.
update(G, T) // Update G using the time series segment measurement T.
```

▶ **Classify** $(T, \mathcal{G})$

Input: T – time series segment, $\mathcal{G}$ - set of GNG models for the individual terrain classes

```
𝒩 ← all_neurons(𝒢)                  // Get all neurons in all GNG models.
neighbor ← nearest(𝒩, T)            // Find 1-NN neuron to T among 𝒩.
return label(neighbor)              // Report the label of the neighbor's GNG.
```

▶ **Inference** $(T_{terrain}, \mathcal{G})$

Input: $T_{terrain}$ – time series segment stripped of cost measurements, $\mathcal{G}$ - set of GNG models for the individual terrain classes

```
label ← classify(T_terrain, 𝒢)      // Label T_terrain ignoring power dimension.
neighbor ← nearest(𝒢[label], T_terrain)  // Find nearest neuron in label GNG.
return cost(neighbor) // Report the missing cost dimension of neighbor.
```

missing dimensions are determined from its reference vector. Further, the mechanism is used to predict the traversal costs over the observed terrain by inferring the missing aggregate cost dimension and then applying (6) or (8), respectively, to compute the cost. The procedure is denoted **Inference** in Alg. 1.

4 Results

We report on the achieved results on time series segment classification and traversal cost inference using the time series segment dataset described in Section 2. Two particular setups are considered as follows: 10 s segments with the aggregate costs denoted according to the number of subsampled points as *time series* 100, 50, 25, or 5, i.e., the segments are subsampled with 10, 5, 2.5, and 0.5 Hz, respectively; and the baseline non-time series setup with the mean power over the 10 s period is denoted *mean value*. In the following parts, we report on the terrain classification, cost prediction, and a short discussion of the results.

4.1 Terrain Classification

The classification correctness computed according to (9) is reported in Table 1. The best classification is achieved using the *time series* segments with 25 points and the respective confusion matrix is presented in Table 2. The *time series* segment with 5 points and the baseline non-time series *mean value* setup provide the worst performance among the evaluated classifiers. However, even the worst

Table 1. Classification correctness

Human Label	*Mean value* (Baseline)	*Time series* with # pts 5	25	50	100
flat	63.60 %	58.45 %	84.19 %	75.73 %	71.69 %
cubes	52.83 %	51.34 %	57.61 %	57.91 %	57.31 %
cubes covered with black	75.21 %	67.64 %	79.83 %	80.25 %	78.99 %
black	87.18 %	84.37 %	90.00 %	93.43 %	92.50 %
turf	76.44 %	85.09 %	98.07 %	98.55 %	98.07 %
cubes covered with turf	57.65 %	81.08 %	61.26 %	60.36 %	58.55 %
All	69.47 %	69.33 %	78.97 %	78.30 %	76.81 %

Table 2. Classification confusion matrix for the segments with the *time series* subsampled to 25 points

Human Label	Predicted Label *flat*	*cubes*	*cubes covered with black*	*black*	*turf*	*cubes covered with turf*
flat	229	0	32	11	0	0
cubes	24	193	114	4	0	0
cubes covered with black	39	2	190	7	0	0
black	32	0	0	288	0	0
turf	0	0	0	0	204	4
cubes covered with turf	0	0	0	1	43	68

classifiers may achieve satisfiable performance over specific terrains. For example, *time series* with 5 points is the most precise classifier of *cubes covered with turf*.

Overall, the most of the confusion between the individual terrains appear to be between the visually similar terrains such as *turf* and *cubes covered with turf*, or between the terrains that might exhibit similar shape property or proprioceptive experience. In Fig. 2, the terrain classification is projected onto the selected terrains. Notably, a portion of the terrains that are considered hard to traverse based on human expertise is classified as *flat*, suggesting that the human labels may not be consistent with the robot proprioceptive experience.

4.2 Traversal Cost Prediction

The performance of the traversal cost prediction evaluated using RMSE computed according to (10) is reported in Table 3. The results are similar to the classification since the *time series* with 25 points provides the best prediction, and the *time series* with 5 points provides the worst performance. It is interesting to note that except *flat*, the highest RMSE is over the terrain types *black*

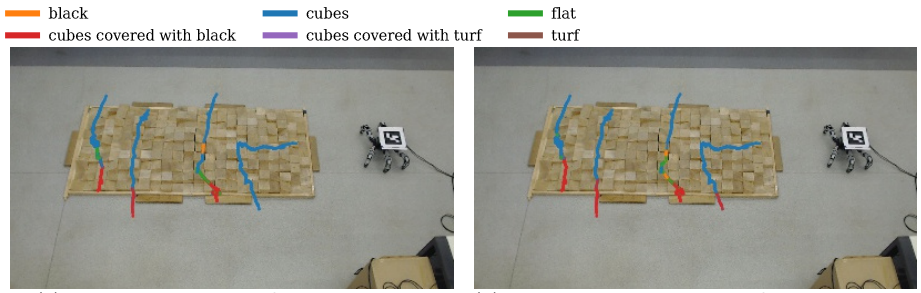

(a) *Time series* 25 classification on *cubes*.

(b) Baseline *mean value* classification on *cubes*.

(c) *Time series* 25 classification on *cubes covered with turf*.

(d) Baseline *mean value* classification on *cubes covered with turf*.

Fig. 2. Terrain classification projected over the selected terrains.

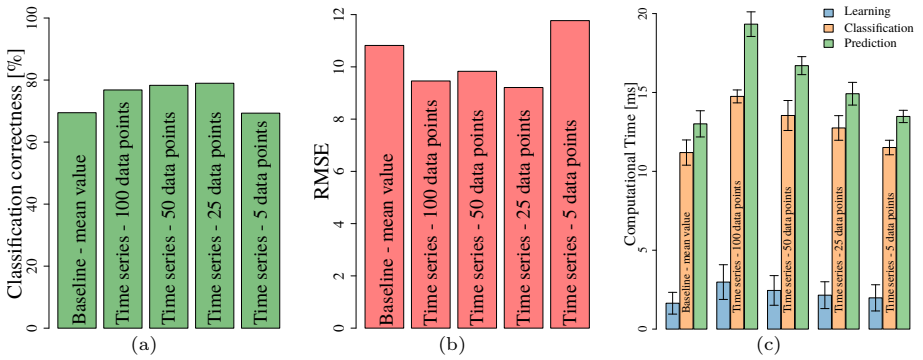

Fig. 3. Overall results for the (a) classification correctness, (b) RMSE of the traversal cost prediction, and (c) the measured execution wall time per one time series segment or non-time series data point using the Intel i5-4460 CPU, 16 GB memory, where the reported values are means of 10 runs.

and *cubes covered with black* with the relatively high classification correctness as reported in Table 1.

4.3 Discussion

The results, aggregated in Figs. 3a and 3b, suggest that the *time series* segments subsampled with 25 points learn better classifiers and predictors than both the

Table 3. Traversal cost prediction RMSE

Human Label	*Mean value* (Baseline)	*Time series* with # pts 5	25	50	100
flat	14.43	14.96	11.63	12.65	10.78
cubes	7.91	8.02	7.90	8.36	8.47
cubes covered with black	12.06	10.77	7.89	9.18	8.42
black	12.68	16.47	11.78	12.09	12.70
turf	5.12	4.95	4.79	5.07	4.78
cubes covered with turf	6.44	5.62	6.19	6.22	5.89
All	10.82	11.77	9.21	9.83	9.46

most dense *time series* with 100 points and the baseline non-time series *mean value*s. According to the wall execution times reported in Fig 3c, the subsampled *time series* are less computationally demanding than the *time series* with 100 points, but they are more demanding than the baseline non-time series *mean values*.

Finally, the reported confusion between the individual terrains in Table 2, and the high RMSE in Table 3 suggest that each terrain label may comprise multiple different robot proprioceptive experience. Therefore, human labels might not be sufficiently descriptive; they are downright misleading. The found observations thus support the results previously reported in [4].

5 Conclusion

In this paper, we investigate the time series representation of the hexapod walking robot terrain traversal dataset. A Growing Neural Gas (GNG) schema is used to classify the traversed terrains and predict energy-based traversal cost. The baseline non-time series setup is outperformed by the proposed time series of terrain descriptors and robot proprioception characterized as the aggregate traversal cost when it is subsampled with at least 2.5 Hz. Overall, the time series subsampled with 2.5 Hz learn the best classifiers and cost predictors among the evaluated classifiers. Moreover, they provide better computational efficiency than time series sampled with higher frequencies, albeit the baseline non-time series method is the fastest one. Finally, the herein presented results also support the previous conclusion that human terrain labels might be misleading when reasoning about the robot traversal experience.

Acknowledgement

The presented work has been supported under the OP VVV funded project CZ.02.1.01/0.0/0.0/16_019/0000765 "Research Center for Informatics". The sup-

port under grant No. SGS19/176/OHK3/3T/13 to Miloš Prágr is also gratefully acknowledged.

References

1. Belter, D., Wietrzykowski, J., Skrzypczyński, P.: Employing Natural Terrain Semantics in Motion Planning for a Multi-Legged Robot. Journal of Intelligent & Robotic Systems **93**(3), 723–743 (2019). DOI: 10.1007/s10846-018-0865-x
2. Brown, D., Webster, G.: Now a stationary research platform, nasa's mars rover spirit starts a new chapter in red planet scientific studies. NASA Press Release (2010)
3. Faigl, J., Čížek, P.: Adaptive locomotion control of hexapod walking robot for traversing rough terrains with position feedback only. Robotics and Autonomous Systems **116**, 136–147 (2019). DOI: 10.1016/j.robot.2019.03.008
4. Faigl, J., Prágr, M.: On unsupervised learning of traversal cost and terrain types identification using self-organizing maps. In: International Conference on Artificial Neural Networks (ICANN). pp. 654–668 (2019). DOI: 10.1007/978-3-030-30487-4_50
5. Faigl, J., Prágr, M.: Incremental traversability assessment learning using growing neural gas algorithm. In: Advances in Self-Organizing Maps, Learning Vector Quantization, Clustering and Data Visualization. pp. 166–176 (2020). DOI: 10.1007/978-3-030-19642-4_17
6. Fišer, D., Faigl, J., Kulich, M.: Growing neural gas efficiently. Neurocomputing **104**, 72–82 (2013). DOI: 10.1016/j.neucom.2012.10.004
7. Fritzke, B.: A growing neural gas network learns topologies. In: Neural Information Processing Systems (NIPS). pp. 625–632. MIT Press (1994)
8. Giguere, P., Dudek, G.: Clustering Sensor Data for Terrain Identification using a Windowless Algorithm. In: Robotics: Science and Systems (RSS). Robotics: Science and Systems Foundation (2008). DOI: 10.15607/RSS.2008.IV.004
9. Kampouraki, A., Manis, G., Nikou, C.: Heartbeat Time Series Classification With Support Vector Machines. IEEE Transactions on Information Technology in Biomedicine **13**(4), 512–518 (2009). DOI: 10.1109/TITB.2008.2003323
10. Keogh, E., Kasetty, S.: On the Need for Time Series Data Mining Benchmarks: A Survey and Empirical Demonstration. Data Mining and Knowledge Discovery **7**(4), 349–371 (2003). DOI: 10.1023/A:1024988512476
11. Kohonen, T.: Self-organizing maps. Springer, 3rd edn. (2001)
12. Kottege, N., Parkinson, C., Moghadam, P., Elfes, A., Singh, S.P.N.: Energetics-informed hexapod gait transitions across terrains. In: IEEE International Conference on Robotics and Automation (ICRA). pp. 5140–5147 (2015). DOI: 10.1109/ICRA.2015.7139915
13. Kragh, M., Jørgensen, R.N., Pedersen, H.: Object Detection and Terrain Classification in Agricultural Fields Using 3d Lidar Data. In: International Conference on Computer Vision Systems. vol. 9163, pp. 188–197. Springer (2015). DOI: 10.1007/978-3-319-20904-3_18
14. Lines, J., Davis, L.M., Hills, J., Bagnall, A.: A Shapelet Transform for Time Series Classification. In: International Conference on Knowledge Discovery and Data Mining (SIGKDD). pp. 289–297. ACM (2012). DOI: 10.1145/2339530.2339579
15. McGhee, R.B., Frank, A.A.: On the stability properties of quadruped creeping gaits. Mathematical Biosciences **3**, 331–351 (1968). DOI: 10.1016/0025-5564(68)90090-4

16. Müller, M. (ed.): Dynamic Time Warping, pp. 69–84. Springer (2007). DOI: 10.1007/978-3-540-74048-3_4
17. Nooralishahi, P., Seera, M., Loo, C.K.: Online semi-supervised multi-channel time series classifier based on growing neural gas. Neural Computing and Applications **28**(11), 3491–3505 (2017). DOI: 10.1007/s00521-016-2247-2
18. Prágr, M., Faigl, J.: Benchmarking incremental regressors in traversal cost assessment. In: International Conference on Artificial Neural Networks (ICANN). pp. 685–697 (2019). DOI: 10.1007/978-3-030-30487-4_52
19. Prágr, M., Čížek, P., Bayer, J., Faigl, J.: Online Incremental Learning of the Terrain Traversal Cost in Autonomous Exploration. In: Robotics: Science and Systems (RSS). vol. 15 (2019). DOI: 10.15607/RSS.2019.XV.040
20. Prágr, M., Čížek, P., Faigl, J.: Cost of Transport Estimation for Legged Robot Based on Terrain Features Inference from Aerial Scan. In: IEEE/RSJ International Conference on Intelligent Robots and Systems (IROS). pp. 1745–1750. IEEE (2018). DOI: 10.1109/IROS.2018.8593374
21. Prágr, M., Čížek, P., Faigl, J.: Incremental Learning of Traversability Cost for Aerial Reconnaissance Support to Ground Units. In: Modelling and Simulation for Autonomous Systems (MESAS). Springer (2018). DOI: 10.1007/978-3-030-14984-0_30
22. Rothrock, B., Kennedy, R., Cunningham, C., Papon, J., Heverly, M., Ono, M.: SPOC: Deep Learning-based Terrain Classification for Mars Rover Missions. In: AIAA SPACE 2016. American Institute of Aeronautics and Astronautics (2016). DOI: 10.2514/6.2016-5539
23. Shen, F., Yu, H., Sakurai, K., Hasegawa, O.: An incremental online semi-supervised active learning algorithm based on self-organizing incremental neural network. Neural Computing and Applications **20**(7), 1061–1074 (2011). DOI: 10.1007/s00521-010-0428-y
24. Stelzer, A., Hirschmüller, H., Görner, M.: Stereo-vision-based navigation of a six-legged walking robot in unknown rough terrain. International Journal of Robotics Research **31**(4), 381–402 (2012). DOI: 10.1177/0278364911435161
25. Wei, L., Keogh, E.: Semi-supervised Time Series Classification. In: International Conference on Knowledge Discovery and Data Mining (SIGKDD). pp. 748–753. ACM (2006). DOI: 10.1145/1150402.1150498
26. Xi, X., Keogh, E., Shelton, C., Wei, L., Ratanamahatana, C.A.: Fast Time Series Classification Using Numerosity Reduction. In: International Conference on Machine Learning (ICML). pp. 1033–1040. ACM (2006). DOI: 10.1145/1143844.1143974
27. Zheng, Y., Liu, Q., Chen, E., Ge, Y., Zhao, J.L.: Time Series Classification Using Multi-Channels Deep Convolutional Neural Networks. In: Web-Age Information Management. pp. 298–310. Springer (2014). DOI: 10.1007/978-3-319-08010-9_33